

Supporting Information

A universal strategy for green and surfactant-free synthesis of noble metal nanoparticles

Experimental section

Synthesis of Pt-NPs/C

3.0 mL H_2PtCl_6 ($7.4 \text{ mg mL}^{-1}\text{Pt}$) was added into the mixed solution containing 20 mL ethylene glycol, 10 mL deionized water, and 51.8 mg Vulcan XC-72 carbon under ultrasonication for over 25 min, followed by adjusting the pH up to 10 using 0.1 M KOH solution. The mixture was bubbled with high-purity nitrogen for 15 min, then heated to 60°C under H_2 bubbling for 2.0 h. The obtained colloidal mixture was centrifuged and washed with deionized water for several times, and the final collected product was named as Pt-NPs/C.

Synthesis of Pd-NPs/C (or Rh-NPs/C)

61.9 mg Na_2PdCl_4 (or 79.7 mg $(\text{NH}_4)_3\text{RhCl}_6$) was added into the mixed solution containing 20 mL ethylene glycol, 10 mL deionized water, and 51.8 mg Vulcan XC-72 carbon under ultrasonication for over 25 min, followed by adjusting the pH up to 10 using 0.1 M KOH solution. The mixture was bubbled with high-purity nitrogen for 15 min, then heated to 60°C under H_2 bubbling for 2.0 h. The obtained colloidal mixture was centrifuged and washed with deionized water for several times, and the final collected product was named as Pd-NPs/C (or Rh-NPs/C).

Electrochemical measurements

2.0 mg Pt-NPs/C was dispersed into a mixture of 0.74 mL ethanol, 0.24 mL deionized water, and 0.02 mL Nafion solution (5 wt%) under ultrasonication for 25 min, then 5.0 μL of the resulting ink was dropped onto a freshly polished glassy carbon rotating disk electrode (RDE, 5 mm in diameter) for the subsequent electrochemical tests. The Pt loadings of Pt-NPs/C and Com Pt/C on the RDE surfaces are respectively 15.1 and 15.3 $\mu\text{g cm}^{-2}\text{Pt}$. All electrochemical measurements were operated on an electrochemical workstation (Metrohm Autolab PGSTAT302N). A graphite rod and Hg/HgSO_4 (with saturated K_2SO_4 solution) were used as the counter and reference electrodes,

respectively. CV curves were tested in nitrogen saturated 0.1 M HClO₄ solution with a scan rate of 50 mV s⁻¹. LSV curves of Pt-NPs/C and Com Pt/C were measured in O₂ saturated 0.1 M HClO₄ solution at 1600 rpm with a scan rate of 5 mV s⁻¹. Additionally, LSV curves of Pd-NPs/C and Com Pd/C were measured in O₂ saturated 0.1 M HClO₄ solution at 1600 rpm with a scan rate of 5 mV s⁻¹. Electrochemical stability of samples in this work was measured using accelerated durability test (ADT) through continuous cycling between 0.6 and 1.1 V (vs. RHE).

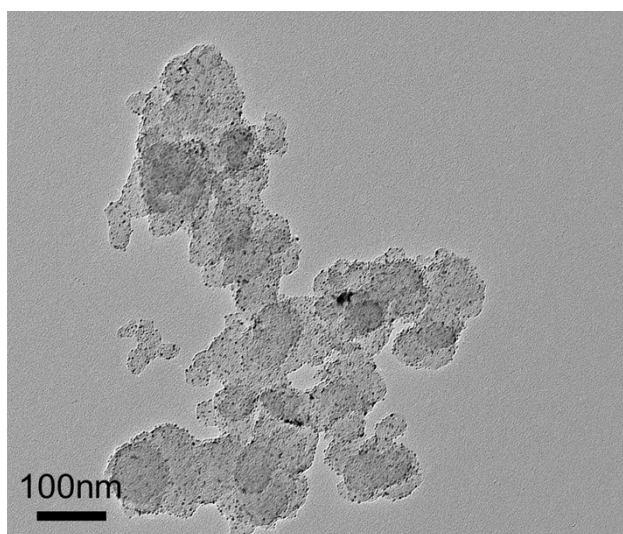


Fig. S1. TEM image of Pt-NPs/C.

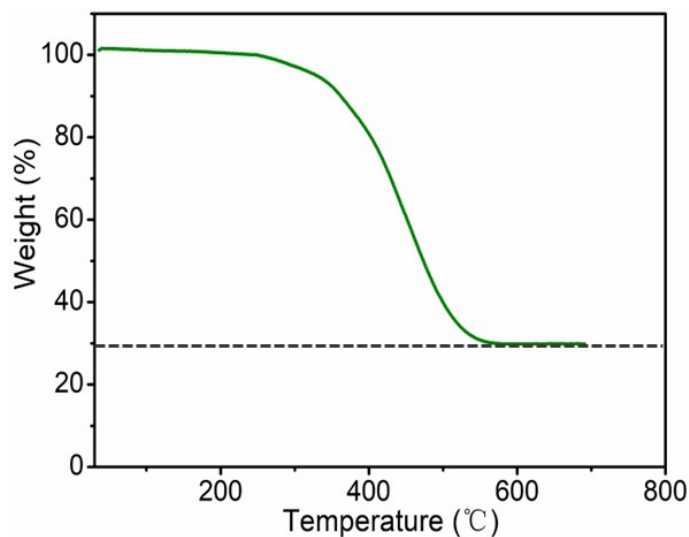


Fig. S2. TGA curve of Pt-NPs/C.

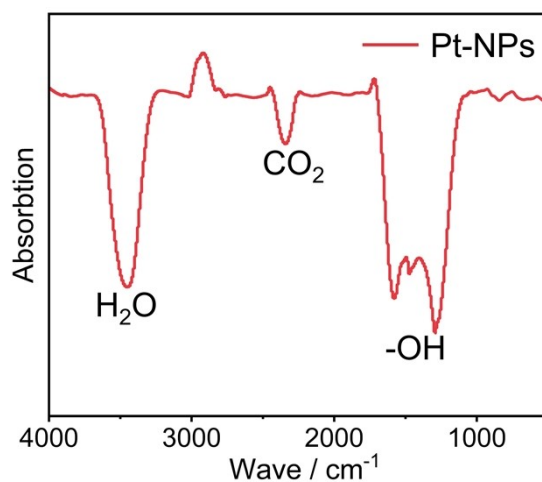


Fig. S3. Fourier transform ir spectrum of Pt-NPs.

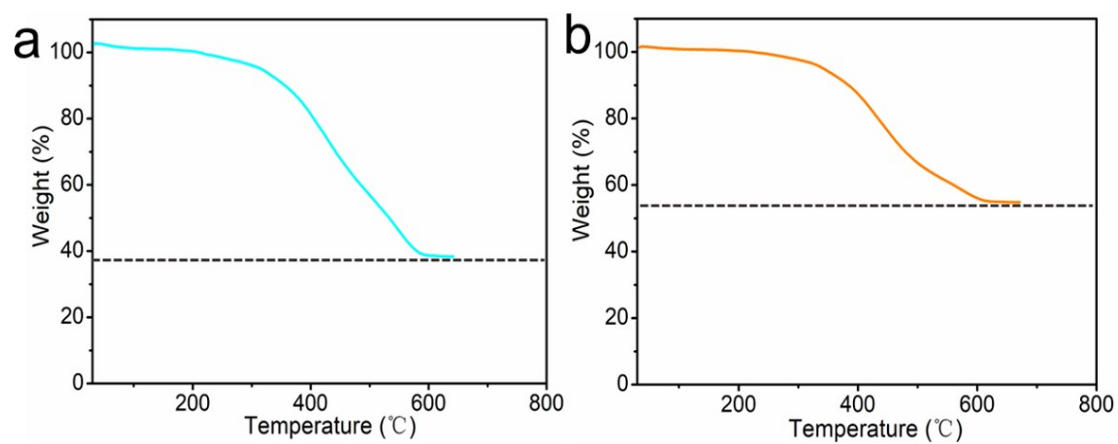


Fig. S4. TGA curve of Pt-NPs/C with Pt loading of (a) 38.4% and (b) 54.7%.

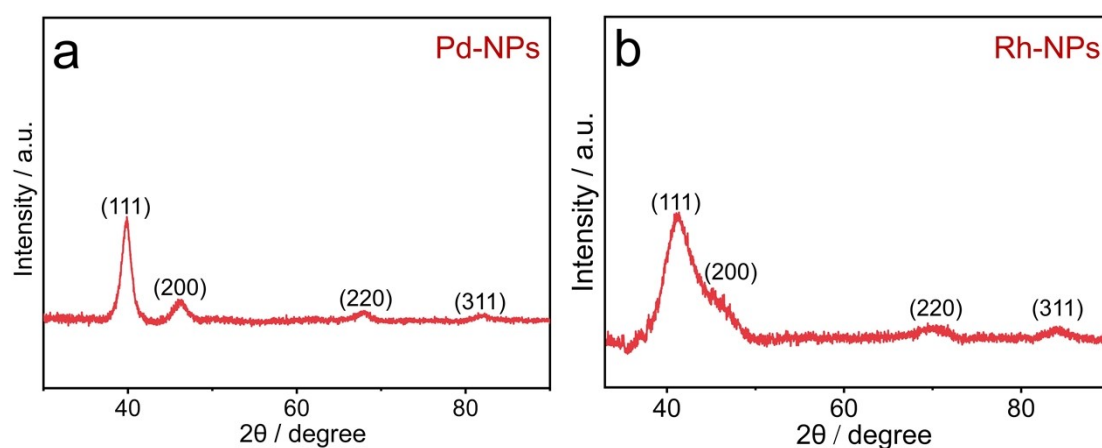


Fig. S5. XRD patterns of (a) Pd-NPs/C and (b) Rh-NPs/C.

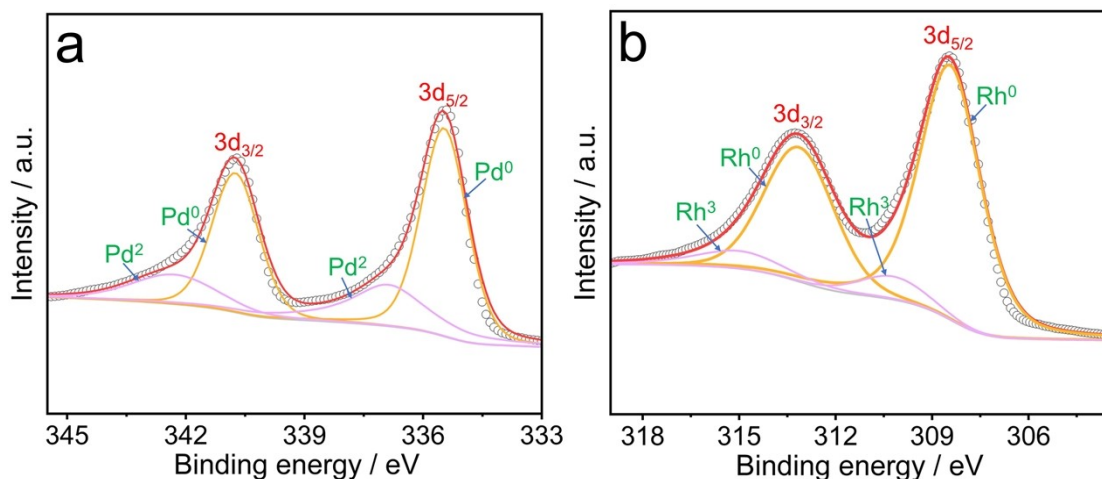


Fig. S6. (a) Pd 3d XPS spectrum of Pd-NPs/C and (b) Rh 3d XPS spectrum of Rh-NPs/C.

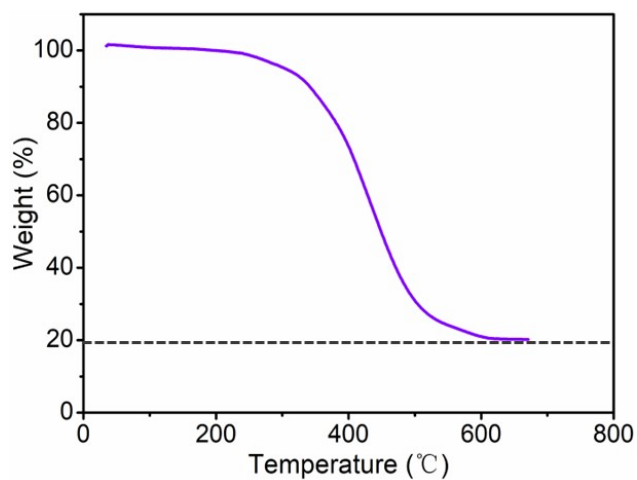


Fig. S7. TGA curve of the prepared Pt-NPs/C in the absence of deionized water.

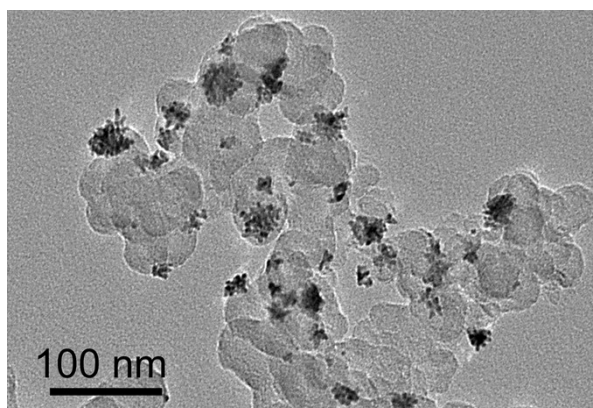


Fig. S8. TEM image of the Pt-based product by replacing ethylene glycol with ethanol.

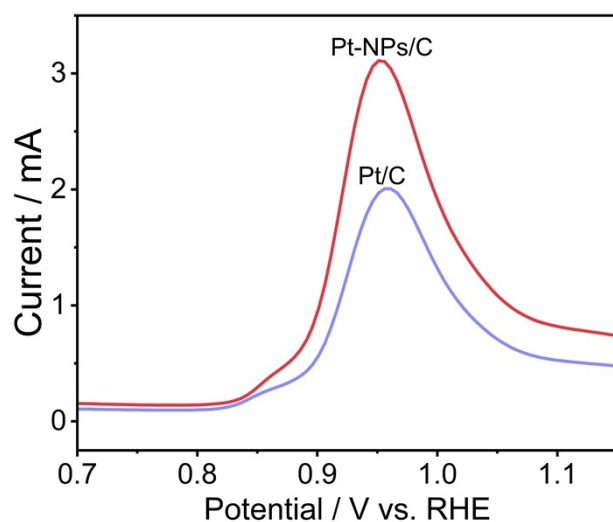


Fig. S9. CO-stripping curves of Pt-NPs/C and Com Pt/C in 0.5 M H₂SO₄ electrolyte at a scan rate of 50 mV s⁻¹.

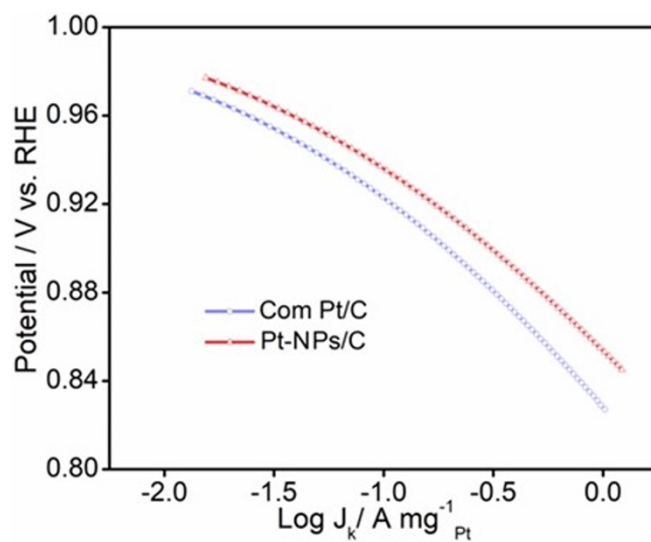


Fig. S10. Tafel plots of Com Pt/C and Pt-NPs/C.

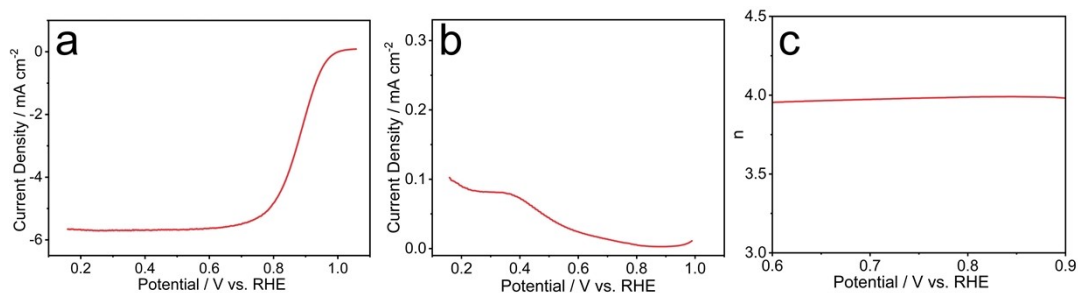


Fig. S11. (a) Disk and (b) ring current densities, as well as (c) the electron transfer number for Pt-NPs/C, at 1600 rpm in 0.1 M HClO₄ solution.

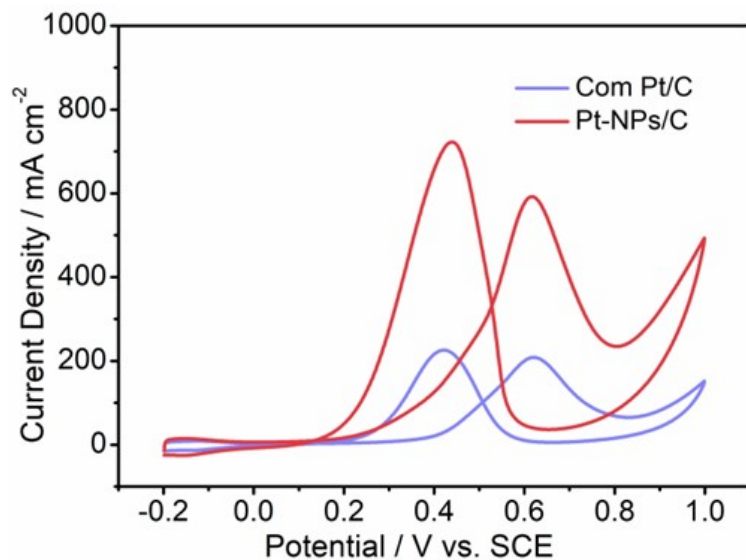


Fig. S12. CV curves of Pt-NPs/C and Com Pt/C in $\text{H}_2\text{SO}_4 + 0.5 \text{ M CH}_3\text{OH}$ electrolyte. Scan rate: 50 mV s^{-1} .

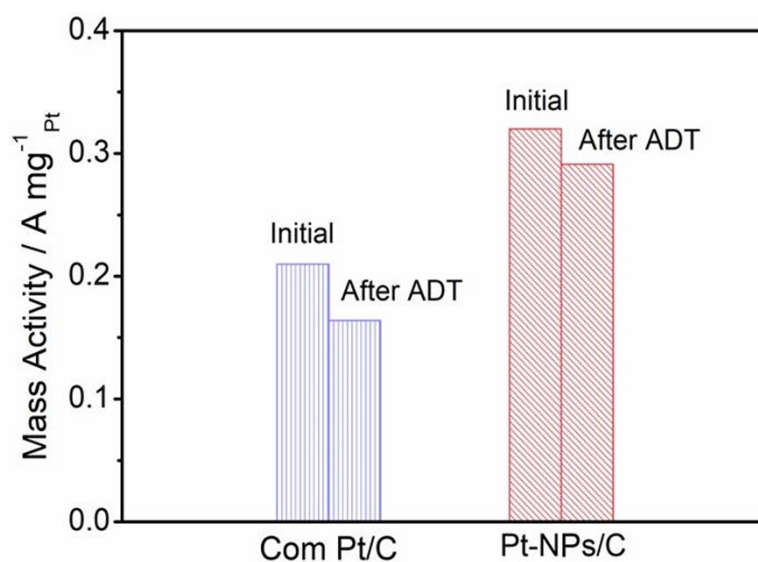


Fig. S13. Mass activity comparison for Com Pt/C and Pt-NPs/C before and after ADTs.

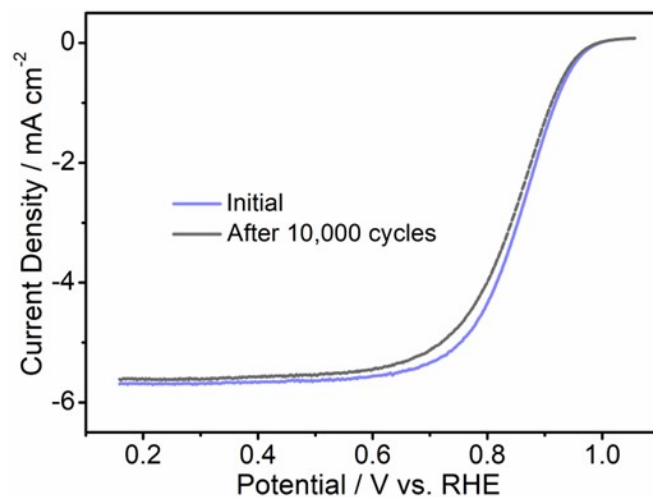


Fig. S14. LSV curves of Com Pt/C before and after 10,000 cycles.

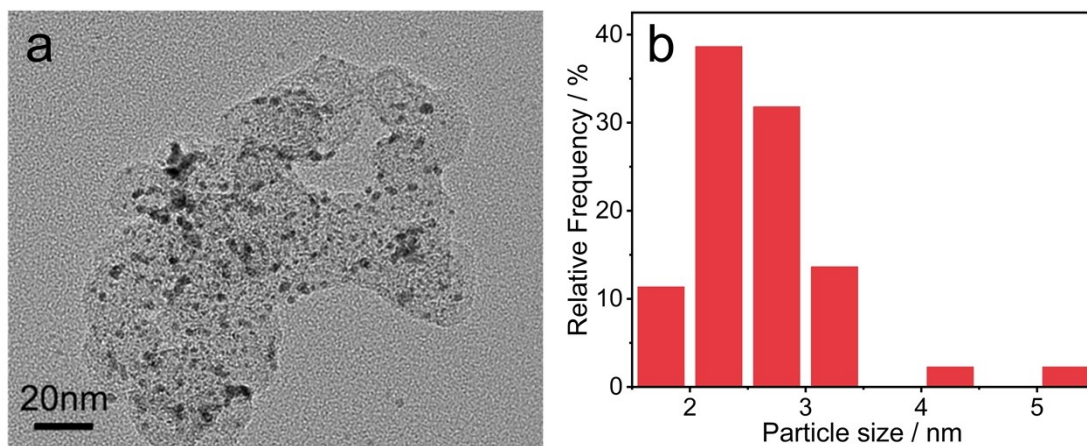


Fig. S15. (a) TEM image Pt-NPs/C after stability testing and corresponding (b) particle size distribution.

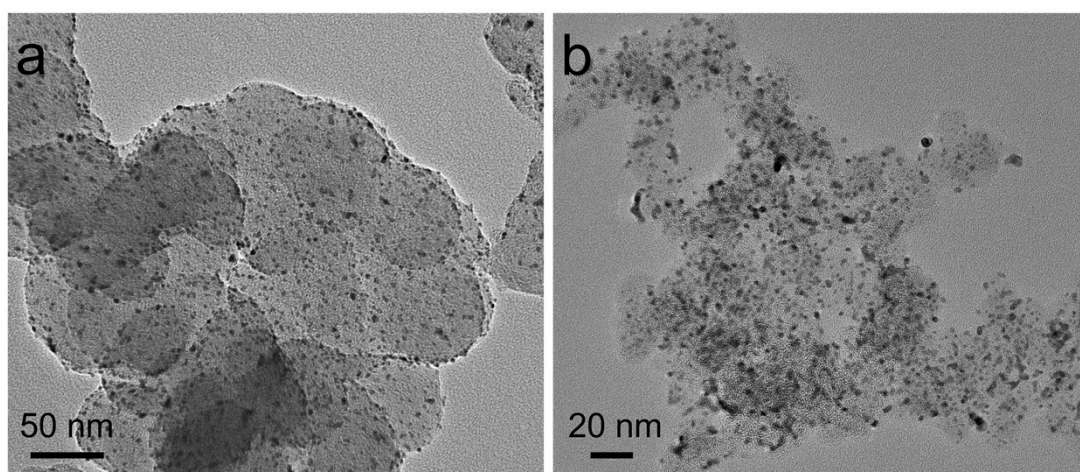


Fig. S16. TEM images of Pt-NPs/C heated at (a) 200°C and (b) 250°C for 1 h in nitrogen atmosphere.

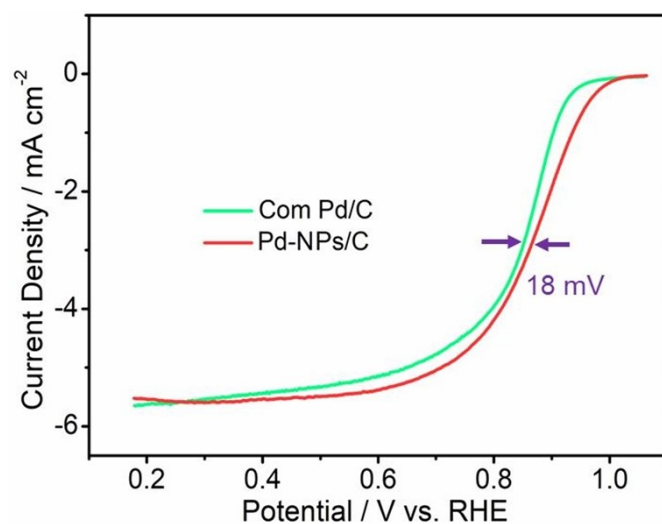


Fig. S17. LSV curves of Com Pd/C and Pd-NPs/C.

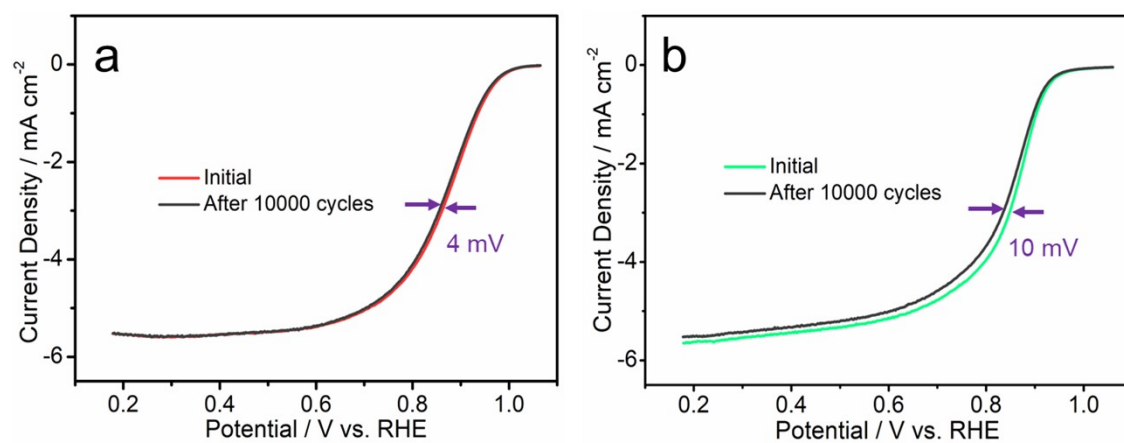


Fig. S18. LSV curves of (a) Pd-NPs/C and (b) Com Pd/C before and after 10,000 cycles.

Table S1. The comparison of specific activity, half-wave potential, and stability between Pt-NPs/C and reported Pt-based nanostructures.

Catalyst	Specific activity (mA cm ⁻²)	Half wave potential (V)	Half wave potential decay after 10000 cycles (mV)	Reference
Pt NPs/TiO ₂ /CSCNT	—	0.871	-9	1
W@Pt/C	0.052	0.846	—	2
Pt&Fe ₂ O ₃ /NC	—	0.862	—	3
Pt@PCNFs	—	0.850	-18	4
10%-Pt-COF900	—	0.848	-60	5
Pt/N-CST	0.169	0.890	-9	6
PtZrNi	0.970	0.880	—	7
PtNi nanowires	0.238	0.799	-20	8
Pt-NiO@Ni	0.263	0.896	-3	9
PtCo@PtIr	0.263	0.926	-9	10
Pt@C/C	0.255	0.887	0	11
Pt/TiO ₂ (OV)-C	0.095	0.862	-5	12
Pt/Zn-BDC	—	0.814	-5	13
Ru-Pt ₂ CoNi/C	1.600	0.873	-15	14
FePt-HMCS	—	0.750	-21	15
Com Pt/C	0.265	0.855	-12	This work
Pt-NPs/C	0.290	0.879	-5	This work

- 1 F. Ando, T. Tanabe, T. Gunji, T. Tsuda, S. Kaneko, T. Takeda, F. Matsumoto, Improvement of ORR activity and durability of Pt electrocatalyst nanoparticles anchored on TiO₂/cup-stacked carbon nanotube in acidic aqueous media. *Electrochim. Acta*, 2017, **232**, 404-413.
- 2 Y. Wang, Y. Yang, L. Zou, Q. Huang, Q. Li, Q. Xu, Yang, H. Carbon-Supported W@Pt Nanoparticles with a Pt-Enriched Surface as a Robust Electrocatalyst for Oxygen Reduction Reactions. *ChemistrySelect*, 2018, **3**(4), 1056-1061.
- 3 H. J. Zhang, Z. Zhou, L. Jia, Z. F. Ma, Y. Xue, Collaborative Anchoring of Pt Nanoparticles and Metal Oxide Nanoparticles on N-Doped Carbon as Catalysts for

- Oxygen Reduction. *ACS Appl. Nano Mater.*, 2023, **6**(14), 13314-13319.
- 4 X. Li, G. Li, C. Deng, L. Jing, C. Feng, Y. Kong, C. He. Constructing ultrafine Pt nanoparticles anchored on N-doped porous carbon nanofibers for efficient and stable oxygen reduction reaction. *Sci. China Mater.*, 2023, **66**(9), 3509-3519.
 - 5 M. Zhou, M. Liu, Q. Miao, H. Shui, Q. Xu, Synergetic Pt Atoms and Nanoparticles Anchored in Standing Carbon-Derived from Covalent Organic Frameworks for Catalyzing ORR. *Adv. Mater. Interfaces*, 2022, **9**, (26), 2201263.
 - 6 J. Cai, J. Chen, Y. Chen, J. Zhang, S. Zhang, Engineering carbon semi-tubes supported platinum catalyst for efficient oxygen reduction electrocatalysis. *iScience*, 2023, **26**, 5.
 - 7 S. Zeng, J. Zhang, H. Wang, X. Zhang, H. Hou, Y. Bai, G. Zhang, Zeng S, Zhang J, Wang H, Ternary PtZrNi nanorods for efficient multifunctional electrocatalysis towards oxygen reduction and alcohol oxidation. *J. Colloid Interf. Sci*, 2023, **638**, 901-9072.
 - 8 W. H. Chen, M. Chang, T. W. Wang, M. S. Wang, Electrospun bimetallic PtNi nanowires as electrocatalyst for oxygen reduction reaction in PEMFCs. *Int. J. Hydrogen. Energy*, 2023. DOI: org/10.1016/j.ijhydene.2023.07.245.
 - 9 F. Zhang, R. Ji, X. Zhu, H. Li, Y. Wang, J. Wang, H. Lan, Strain-Regulated Pt–NiO@Ni Sub-Micron Particles Achieving Bifunctional Electrocatalysis for Zinc–Air Battery. *Small*, 2023, 2301640
 - 10 S. Zhu, Y. Liu, Y. Gong, Y. Sun, K. Chen, Y. Liu, R. Wang, Boosting Bifunctional Catalysis by Integrating Active Faceted Intermetallic Nanocrystals and Strained Pt–Ir Functional Shells. *Small*, 2023, 2305062.
 - 11 Y. Jiang, Y. Wang, J. Qian, Y. Mu, Z. Li, T. Zhao, L. Zeng, Durable carbon-shell-encapsulated Pt/C catalysts synthesized by direct pyrolysis of Pt-pyrrole complexes for the oxygen reduction reaction. *Int. J. Hydrogen. Energy*, 2023. DOI: org/10.1016/j.ijhydene.2023.06.328.
 - 12 Z. Wang, X. Jin, F. Chen, X. Kuang, J. Min, H. Duan, J. Chen, Oxygen vacancy induced interaction between Pt and TiO₂ to improve the oxygen reduction performance. *J. Colloid Interf. Sci.*, 2023, **650**, 901-912.
 - 13 Y. Wang, W. Zhou, Y. Shuai, T. Zhang, P. He, A. Wu, Y. Liu, Tuning the Pt-N coordination in Pt/MOFs nanosheets under N₂ plasma for enhanced oxygen reduction reaction. *J. Alloys Compd.*, 2023, **968**, 171915.
 - 14 P. Mukherjee, I. M. Patil, M. Lokanathan, H. Parse, B. Kakade, A. Swami, Ru decorated Pt₂CoNi/C nanoparticles as a proficient electrocatalyst for oxygen reduction reaction. *J. Alloys Compd.*, 2022, **918**, 165520.
 - 15 C. Yang, H. B. Wang, Liang, P, B. F. Wu, L. Zhao, P. S. Leng, H. Wang, Size and structure tuning of FePt nanoparticles on hollow mesoporous carbon spheres as efficient catalysts for oxygen reduction reaction. *Rare Metals*, 2023, **42**, 1865-1876.